ELSEVIER

Journal of Power Sources 86 (2000) 432–441

JOURNAL OF POWER SOURCES

www.elsevier.com/locate/jpowsour

Pre-reforming of natural gas in solid oxide fuel-cell systems

R. Peters *, E. Riensche, P. Cremer

Institute for Materials and Processes in Energy Systems IWV 3: Energy Process Engineering, Forschungszentrum Jülich, Jülich D-52425, Germany

Accepted 18 October 1999

Abstract

Several measures concerning fuel processing in a solid oxide fuel cell (SOFC) system offer the possibility of significant cost reduction and higher system efficiencies. For SOFC systems, the ratio between internal and pre-reforming has to be optimized on the basis of experimental performance data. Furthermore, anode gas recycling by an injector in front of the pre-reformer can eliminate the steam generator and the corresponding heat of evaporation. A detailed study is carried out on pre-reforming in a reformer of considerable size (10 kW_{el}). Simulating anode gas recycling with an injector, the influence of carbon dioxide on reactor performance was studied. Also, the dependence of the methanol conversion on mass flow and temperature will be discussed. In addition, some results concerning the dynamic behaviour of the pre-reformer are given.

Keywords: Steam reforming; Pre-reformer; Anode gas recycling; Solid oxide fuel cells

1. Introduction

Solid oxide fuel cells (SOFCs) convert the chemical energy of the fuel gas directly to electrical energy. Therefore, they can theoretically achieve high electrical efficiencies. SOFCs operate at temperatures between 700°C and 950°C using H_2-containing gas mixtures as the fuel and O_2 in the air as the oxidant. The high operating temperature of SOFC opens up good possibilities for co-generation applications. The most interesting fuel for SOFC systems used for stationary applications is natural gas consisting mainly of methane. The H_2/CO-rich gas can be advantageously produced by steam-reforming from natural gas consisting of 85% methane. The direct electrochemical conversion of CH_4 in an SOFC is an additional option, although is not feasible at present. The steam-reforming process has to be incorporated into the energy balance as part of the SOFC system.

In order to reach a high total plant efficiency related to low energy consumption and low investment costs, a process concept has been developed based on all the components of the SOFC system. Plant optimization, therefore, requires a tool which takes the characteristic behaviour of stack and peripheral and their interaction into account. An energetic and economic analysis of a decentralized natural gas-fuelled SOFC power plant with 200 kW_{el} capacity was carried out by Riensche et al. [1,2] and Unverzagt [3]. Starting from a basic plant concept with a simple flow sheet and a basic set of SOFC operation parameters and economic data, they performed flow sheet and parameter variations of the plant concept to optimize the cost of electricity (COE) and the plant efficiency. A major target in the process development is to reduce the large amount of air supplied to the fuel cell stacks, which is necessary to remove the electrochemical waste heat. Alternative stack cooling concepts are necessary to improve plant operation.

The endothermal steam-reforming of natural gas within the anode chamber of the SOFC stack is favourably applied to reduce the expense of a pre-reformer and to provide additional cooling of the cell. Internal steam reforming is an attractive option offering a significant cost reduction and higher system efficiencies for an SOFC power plant. Complete internal reforming can lead to carbon formation in the anode chamber and to large temperature gradients in the stack caused by a strong cooling effect of the very fast reforming reaction in the fuel inlet area as was reported previously [4–6]. Because of the higher level of hydrocarbons in natural gas and several problems related to complete internal reforming, a pre-reformer has to be provided in any future SOFC-plant concept development. The concept considered in this work envisages performing the reforming process by two steps

* Corresponding author. Tel.: +49-2461-61-4260; fax: +49-2461-61-8163; e-mail: ra.peters@fz-juelich.de

0378-7753/00/$ - see front matter
PII: S0378-7753(99)00440-1

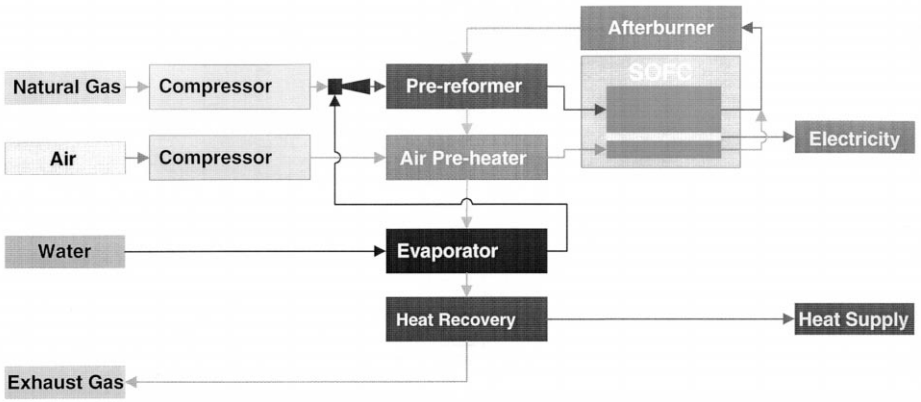

Fig. 1. Basic concept of an SOFC-combined heat and power plant.

in different components, i.e., in a pre-reformer and within the anode chamber of the SOFC stack (internal reforming).

A compact pre-reformer integrating a fuel pre-heater and the steam reformer in one apparatus was designed, built and tested [4]. In a first approach, the influence of process parameters, such as process gas temperature and outflow mass flow on the product steam composition of pre-reforming, was examined under conditions of practical relevance. The SOFC system requirements [1] for the pre-reformer are examined in more detail, studying reformer performance under these conditions.

In Section 2, the basic flow sheet of an SOFC system is described and the flow sheet variation for the steam reforming process is discussed. In Section 3, the experiments performed for the proposed processes are described. In Section 4, the results are discussed together with their feedback on the SOFC system.

2. Balance of plant

The balance of plant calculations were performed by Riensche et al. [1,2] and Unverzagt [3] to describe the sensitivity of cell parameter values on the COE. For the energy analysis of a small-sized combined heat and power SOFC plant, the commercial flow sheet simulator PRO/II (Sim/Sci) was used. This program simulates the mass flow and calculates the energy demand of the common peripheral units. In Section 3, a brief summary of the results is given.

In Fig. 1, the flow sheet of a basic plant concept is shown. The natural gas stream (400 kW LHV) is compressed to overcome the pressure losses in the components. Before entering the pre-reformer, it is mixed with steam ($H_2O/C = 2.5$ mol/mol) produced in a heat-integrated boiler. The pre-reformer is heated recuperatively by the hot gas leaving the afterburner. The large air stream requires an energy demand of 41 kW for compression. The air is then preheated recuperatively to 1123 K. In the SOFC stack, a gross electric DC power of 231 kW is produced. After subtracting the energy loss of the inverter and the energy demand for compression, a net AC power output of 172 kW remains. Thus, the electrical plant efficiency is 43%. Taking into account the useful heat of 94 kW additionally produced a total plant efficiency of 67% is reached. These are the values of the simple unoptimized base case of the assumed 200 kW SOFC plant.

Instead of external steam production in the base case (Fig. 1), steam produced in the electrochemical reaction of the fuel cell can be used when part of the hot anode outlet gas is recycled to the pre-reformer inlet. Gas recycling can be realized with blowers, hot gas fans or injectors.

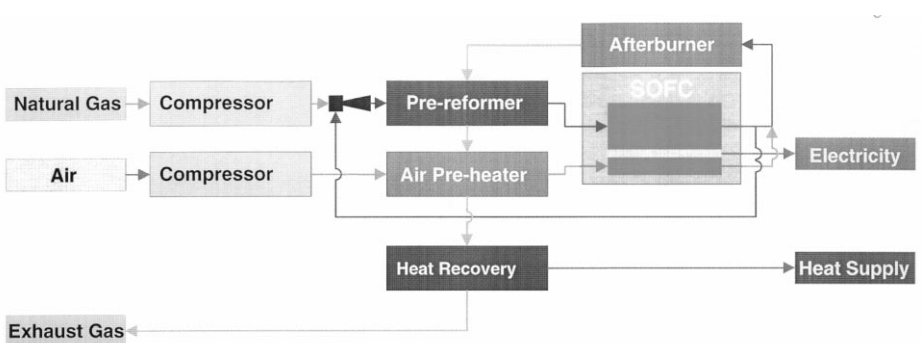

Fig. 2. Anode gas recycling with an injector.

Table 1
Inflow gas composition with anode gas recycling given by the flow sheet simulation
Molar ratio steam: natural gas (NG): 2.5. $R_{recycling}$: ratio of recycled and fresh gas.

Mix	y_{NG} / %	y_{H_2O} / %	y_{CO} / %	y_{CO_2} / %	y_{H_2} / %	$R_{recycling}$
A	18	45	6	21	10	5.2
B	20	49	3	24	4	4.3
C	20	50	2	24	4	4.4
D	17	43	7	20	13	5.1
E	19	47	4	23	7	4.3

A certain steam/carbon ratio at the pre-reformer inlet is required to overcome the carbon formation limits. As in the base case, a ratio of $H_2O/C = 2.5$ was chosen for the flow sheet shown in Fig. 2. This ratio defines the recycle ratio. An analysis of the calculations shows that many peripheral and stack-operating parameters are influenced when the plant design is changed to recycle anode gas. The major advantages are the following.

(a) No external steam production.

(b) Stack fuel utilization (one pass through the stack) is reduced from 80% to about 60% (the value of plant fuel utilization remains fixed at 80%); thus, the cell area is lowered by about 25%.

(c) The exhaust gas has a lower steam concentration, so that the unusable heat content (last cooling step between about 80°C and room temperature) is lower and consequently, the total plant efficiency (including useful heat) is higher.

The disadvantage is that a higher compression energy for the natural-gas-driven injector is necessary. All these effects result in a COE reduction of 7% for the concept of Fig. 2 compared to the base case in Fig. 1. In a plant concept with external steam generation, the exhaust gas contains this excess steam in addition to the steam produced. A good deal of heat remains unused, since below 80°C, condensation takes place outside the plant. Anode gas recycling provides an internal steam circuit. Therefore, the steam concentration in the exhaust gas and the corresponding heat loss is reduced. Furthermore, the temperature increase in the afterburner is higher in the case of lower steam contents in the fuel cell outlet gases, so that the ratio of the unused to the used enthalpy flow of the exhaust gas becomes smaller. Both effects result in a higher total plant efficiency of 81% instead of 67% in the base case. A further improvement of the heat management up to an efficiency of 93% can be achieved in the case of complete internal steam reforming if the air ratio for the exhaust burner is reduced from 3.6 to 1.3.

The SOFC plant flow sheets calculated by Riensche and Fedders [7] also have to be checked by experiments pertaining to the reforming process. The effect of anode gas recycling on the pre-reforming step and on internal reforming has to be examined by measurements of catalyst activity. For a small-scale CHP SOFC plant, work concerning the pre-reformer is focused on:

(a) gas processing on the fuel side for reforming natural gas with steam and reforming natural gas with steam and carbon dioxide (in the case of anode gas recycling); and

(b) gas processing in the stack peripherals for a recuperative heat exchange for fuel preheating and steam production, and recycling water to the anode inlet by anode gas recycling.

The outflow concentrations resulting from the balance of plant calculations by Riensche and Fedders [7] are given in Table 1.

3. Experimental

In order to simulate the critical gas processing steps of an SOFC plant under realistic operating conditions, a test facility for peripheral components was constructed.

Components like pre-reformers, injectors and heat exchangers have been developed and investigated. The capacity of the test facility corresponds to a 10-kW SOFC plant. The pre-reformer and other peripheral components are located in a pressure vessel (Fig. 3). As the heat source, a natural gas burner is mounted on top of the pressure vessel. The test facility is designed for system pressures up to 14 bar and burner temperatures up to 1000°C. Reforming experiments were performed using pipeline natural gas. Desulphurization took place in an

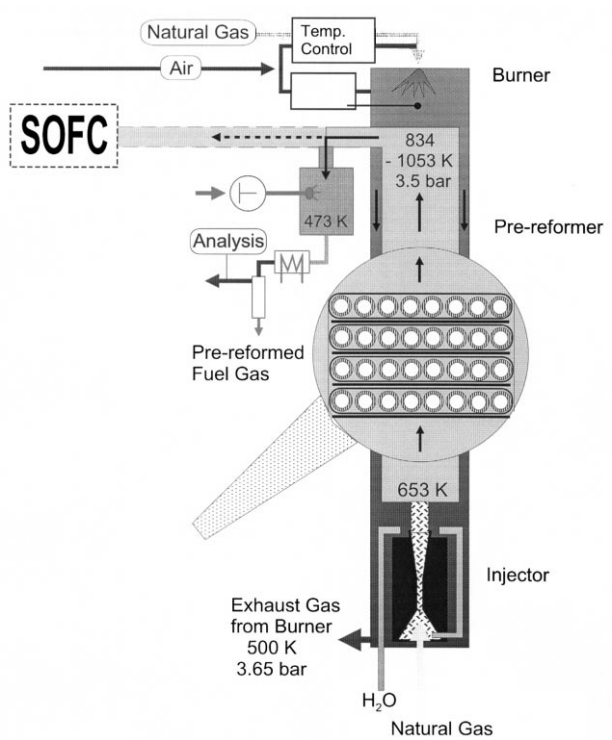

Fig. 3. Test facility for peripheral components.

active carbon bed. The composition of the natural gas was: 88.33% (mol) CH_4, 5.50% C_2H_6, 1.30% C_3H_8, 0.46% C_4H_{10}, 0.11% C_5H_{12}, 0.10% higher hydrocarbons, 2.95% nitrogen and 1.25% carbon dioxide. The product gas of the pre-reformer is cooled down to condense out steam. The composition of the dry gas is analysed by means of gas chromatography (Hewlett Packard Series II 5890). For detection of ethane contents of the order of 1 mol% (ethane content in the natural gas 5.5 mol%), the gas chromatograph was calibrated with a standard gas composition. The main components were checked by an IR Binos Analyzer system. In order to perform a mass balance for the pre-reformer, the following flow rates were measured: the flow rate of water and natural gas before entering the pre-reformer and the flow rates of carbon dioxide, carbon monoxide and hydrogen in the case of anode gas recycling.

Instead of a fuel preheater and a conventional reformer, which would be relatively large, only one apparatus for simultaneous fuel preheating and natural gas reforming is used in the compact pre-reformer concept. Conventional reformers are optimized for high methane conversions and consist of reformer tubes about 10 m in length [8].

A pre-reformer was constructed by using a simple plate heat exchanger. As shown in Fig. 4, the space between adjacent walls is filled with one layer of a conventional

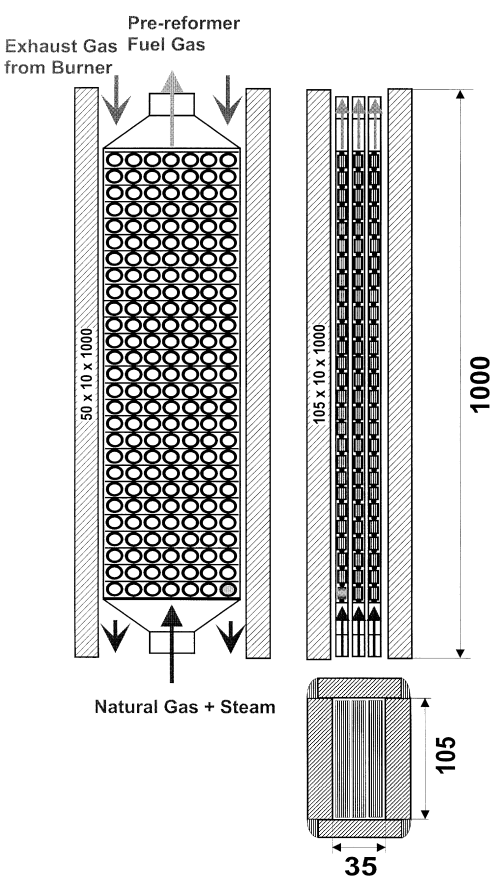

Fig. 4. Compact pre-reformer with Raschig rings.

Table 2
Adiabatic burner temperatures for given air ratio

Air ratio, λ	Adiabatic temperature (K)
3	1141
3.25	1083
3.5	1033
3.75	989
4	950

Raschig ring steam reforming catalyst (Südchemie G-90 B, $12 \times 6 \times 6$ mm^3). Experiments were carried out at a pressure of 3.5 bar. In front of the pre-reformer, a heat exchanger was built and mounted to preheat the mixture consisting of natural gas and water, subsequently to evaporate the water and to superheat the steam–natural gas mixture. The heat required by the evaporator/heat exchanger unit was provided by the exhaust gas from the burner leaving the pre-reformer.

A control strategy for the burner unit was implemented, regulating the natural gas flow to the burner for the heat required by the evaporator/heat exchanger unit and the pre-reformer in such a way that the temperature at the evaporator outlet on the exhaust gas side amounted to 498 K (data series 97) and 510 K (data series 99), respectively. In addition, the temperature on the process side of the pre-reformer was controlled by the air ratio of the air–natural gas mixture entering the burner.

Table 2 shows the adiabatic burner temperatures for given air ratios. The adiabatic temperature varies from 950 K at $\lambda = 4$ up to 1141 K at $\lambda = 3$.

Analysing the experimental data, the exhaust gas temperature after the burner amounts to 834–1075 K. The entrance temperature of the exhaust gas into the evaporator/heat exchanger unit is 735–809 K. The exhaust gas leaving the evaporator/heat exchanger unit has a temperature of between 498 and 511 K. On the other hand, the natural gas–water mixture was fed into the evaporator/heat exchanger at 373 K (data series 97; 382 K data series 99) and leaves the evaporator as a steam–natural gas mixture with a temperature of between 625 and 682 K. The process gas temperatures at the pre-reformer outlet are between 809 and 1058 K.

At higher temperatures ($T > 975$ K) on the process side, the performance of the pre-reformer cannot be increased linearly due to the influence of the exhaust gas flow on the heat transport coefficients. With increasing pre-reformer temperature, the gas-flow is reduced by decreasing the air ratio. This leads to lower heat transfer coefficients and limits the rate of reaction on the process side.

The methane conversion rate and the CO selectivity were determined by a least squares fit between measured concentrations of the dry product gas and the gas composition calculated from the balances for carbon, hydrogen and

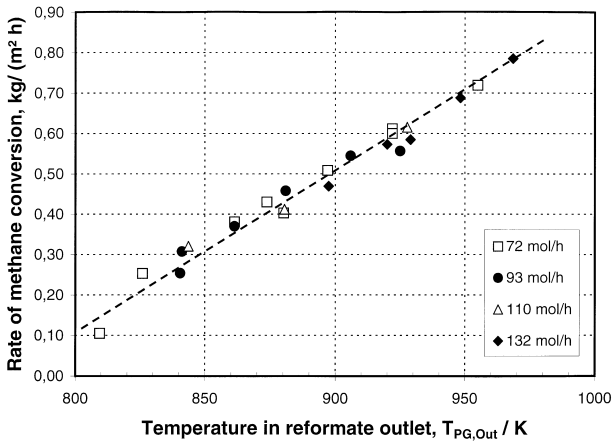

Fig. 5. Conversion rate of methane at different mass flows depending on temperature (Data series 97-1).

oxygen. This procedure had to be followed due to the limited data measured for the pre-reformer.

4. Results and discussion

4.1. Methane and ethane conversion rate

In Fig. 5, the methane conversion rate relative to the wall area between exhaust and process gas is plotted as a function of the temperature at the process gas outlet as proposed in Ref. [4]. At all temperatures, the rate is independent of the mass flow chosen. Within the ranges of the parameters investigated (low and medium methane conversions), the reforming process is completely kinetically controlled. The variation of temperature results in an increase of 0.4 kg CH_4/(h m^2) per 100 K temperature increase. This corresponds to a methane conversion of 42.5% at 955 K and 22.5% at 861 K.

In Fig. 6, the methane and the ethane conversion rates are shown as functions of temperature. It can be seen that the methane conversion rate increases from 6.2% at 810 K to 25% at 969 K. No dependence of the methane conversion rate on the molar flow of natural gas cannot be observed. The ethane conversion rate varies between 40% and 50%. Due to a high scattering among measured data, the temperature dependence of the ethane conversion rate is difficult to determine. The ratio of ethane to methane rate amounts to 7 at 810 K and 1.85 at 969 K. This ratio can be described by an exponential expression depending on temperature. Such a relation was used to calculate the ethane conversion rate for all data points, whereas the ethane concentration could not be measured in the product gas.

4.2. Ageing behaviour

In this section, some aspects of catalyst degradation will be discussed. The experimental results shown in Figs. 5 and 6 cannot be interrelated due to the use of different quantities, i.e., the methane conversion in percent and the specific rate of methane conversion in kilogram per square meter hour [kg/(m^2 h)] relative to the wall area. By analysing the experimental results with similar quantities, it can be seen that the reactor performance decreases from data series 97-1 to 97-2. Fig. 7 shows the rate of methane conversion for both data series as well as additional data series derived from reference data before and after the experiments, with anode gas recycling, i.e., the data series 99-3 before, and the data series 99-5 after CO_2 blending. The data clearly show a decrease in the methane conversion rate between August 97 (data series 97-1) and September 97 (data series 97-2). A further reduction, accompanied by a higher scattering of the data, can be

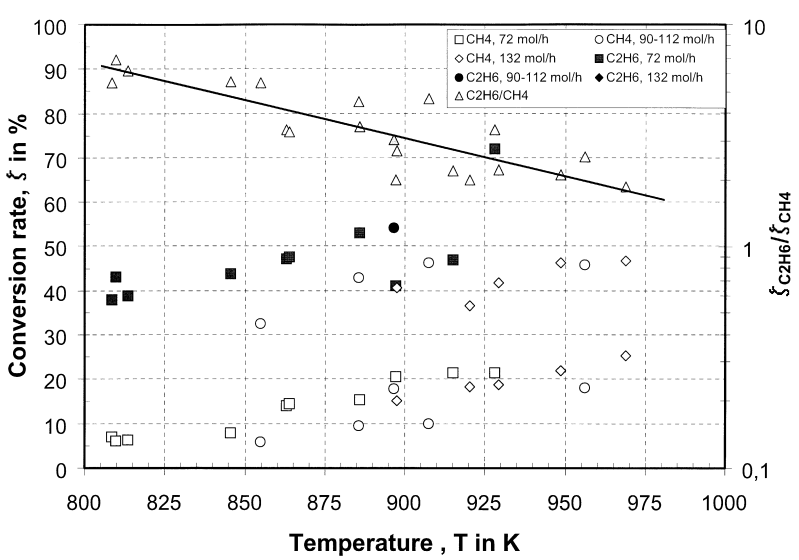

Fig. 6. Methane and ethane conversion rate as a function of temperature for three different molar flows of natural gas (Data series 97-2). (□) ζ_{CH_4}; (■) $\zeta_{C_2H_6}$ for $\dot{n}_{NG}$ = 72 mol/h; (○) ζ_{CH_4}; (●) $\zeta_{C_2H_6}$ for $\dot{n}_{NG}$ = 100 mol/h; (◇) ζ_{CH_4}; (◆) $\zeta_{C_2H_6}$ for $\dot{n}_{NG}$ = 132 mol/h; (△) $\zeta_{C_2H_6}/\zeta_{CH_4}$.

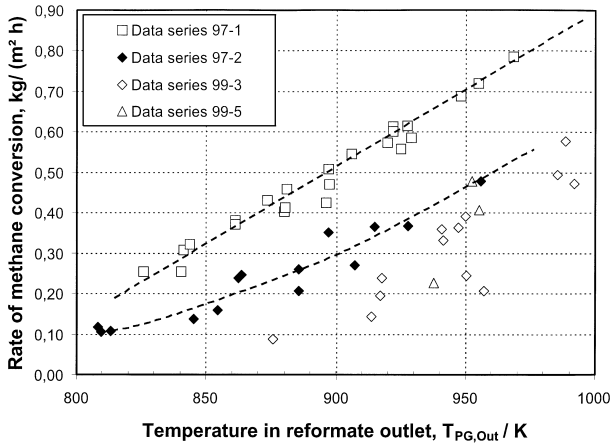

Fig. 7. Conversion rate of methane, different data series depending on temperature (Data series 97-1). Outflow flow of natural gas: 54–132 mol/h.

observed for the measured rates between December 1998 and March 1999 (data series 99-3, data series 99-5). The ageing behaviour is accompanied by a decrease in the temperature difference between exhaust and process gas at the top of the pre-reformer. In the kinetically controlled region, the endothermic reaction leads to a temperature drop in the reaction zone as for the data series 97-1 and 97-2. Such a temperature profile has also been observed for methanol steam-reforming in fixed-bed reactors [9].

Despite the observed ageing effects, the experiments were continued by adjusting a reference flow at the controllers to check the actual rate of methane conversion, without any blending, before mixing CO_2, H_2 or CO into natural gas and steam.

4.3. Influence of anode gas recycling

The central theme of the influence of anode gas recycling on reactor performance is discussed here. The experiments were initiated with carbon dioxide being blended into natural gas and steam.

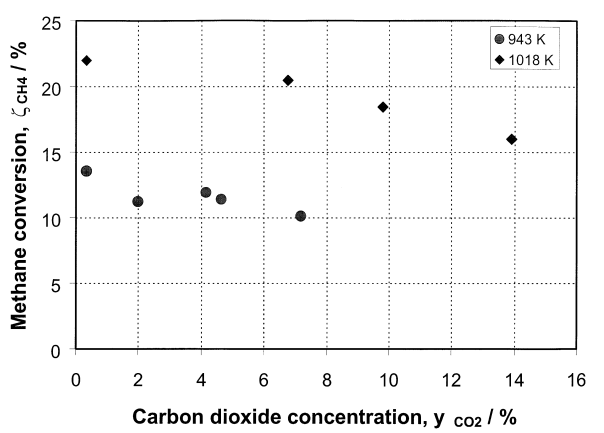

Fig. 8. Effect of carbon dioxide blending on methane conversion rate.

Table 3
Inflow gas composition for simulated anode gas recycling
NG: natural gas. $R_{recycling}$: ratio between recycled and fresh gas.

Mix	y_{NG} / %	y_{H_2O} / %	y_{CO} / %	y_{CO_2} / %	y_{H_2} / %	$R_{recycling}$
A	20.6	58.1	3.1	12.6	5.7	0.97
B	24.0	60.0	2.6	8.4	5.2	0.54
C	24.5	61.1	2.1	8.4	3.9	0.46
D	24.9	62.2	1.3	8.9	2.7	0.43
E	25.3	63.3	0.9	8.9	1.6	0.42
F	25.4	63.6	0.6	8.6	1.7	0.40

Fig. 8 shows the influence on the methane conversion of blending a natural gas–steam mixture with carbon dioxide. As can be seen, the methane conversion rate drops from 22% at the reference state ($y_{CO_2} = 0.34\%$ from natural gas) to 15% at 14% carbon dioxide in the inflow at 1018 K. At 943 K, the methanol conversion decreases with the same slope as at 1018 K.

At 1012 K, blending a natural gas–steam mixture with hydrogen (5.7%) results in an increase of the methane conversion rate by about 9%. On the other hand, blending with carbon monoxide (5.2%) leads to a decrease in methane conversion of about 52% at 963.2 K and about 26% at 1031 K.

Further investigations were made to study the influence of anode gas recycling with inflow mixtures as proposed in Table 1. Unfortunately, such mixtures could not be prepared due to strong reduction in catalyst activity with increasing concentrations of carbon dioxide and carbon monoxide. The resulting methane conversion rates were limited to 8–10% as the lowest values consequent upon the precision of the analytical method.

As can be seen from Table 3, six mixtures were studied, which correspond to carbon dioxide concentrations of half or one third of the values in Table 1. The corresponding recycling ratios are very low due to the fact that only between 50% ($R_{recycling} = 1$) and 70% ($R_{recycling} = 0.4$) of the steam needed is recovered by anode gas recycling. The

Table 4
Pre-reformer performance for simulated anode gas recycling

Mix	T (K)	r_{CH_4} / (kg/h m²)	Δr_{CH_4} / %	$\dot{n}_{NG}$ / (mol/h)	ζ_{CH_4} / %
A	953.3	0.347	−14.6	69.4	21.2
A	1027.5	0.406	−10.7	69.4	24.9
B	962.1	0.194	−52.4	78.2	10.5
B	1011.2	0.327	−11.2	78.2	17.8
C	946.9	0.177	−56.4	78.2	9.6
C	1013.2	0.320	−13.3	78.2	17.3
D	963.1	0.183	−55.0	78.2	9.9
D	1029.0	0.312	−15.5	78.2	16.9
E	945.0	0.197	−51.5	78.2	10.7
E	1013.2	0.341	−7.4	78.2	18.5
F	961.5	0.206	−49.4	78.2	11.2
F	1011.2	0.345	−6.4	78.2	18.7

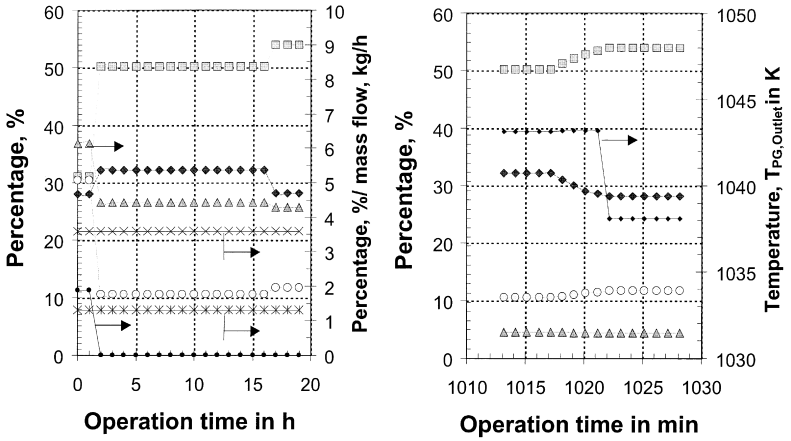

Fig. 9. Product gas composition after a change in outflow gas composition from 13.7% CO_2, 22.79% natural gas, 63.5% H_2O to 26.9% natural gas and 63.10% H_2O at a molar flow of 71.16 $mol_{natural\ gas}/h$. (□) H_2; (♦) CH_4; (○) CO_2; (▲) CO; (×) $\dot{m}_{H_2O}$;(*) $\dot{m}_{NG}$; (·) $\dot{m}_{CO_2}$; (♦) $T_{process\ gas\ outlet}$.

residual steam has to be provided by evaporating water. In Table 4, the pre-reformer performance for simulated anode gas recycling is given at two temperatures in comparison to the data without blending, i.e., $\Delta r_{CH_4}/\%$. The reduction in catalyst activity is more pronounced at lower temperatures, i.e., at 950 K. The methane conversion was, in nearly all cases, halved compared to the conversion without blending. In the case of the first value, it has to be considered that this was the first experiment with a mixture shown in Table 3. At 1013 K, all the mixtures show a reduction of methane conversion of about 6 to 16%.

A further effect of carbon dioxide on the reactor performance can be observed after a change in outflow gas composition. Fig. 9 shows the dry product gas composition after a change from a mixture consisting of 13.7% CO_2, 22.79% natural gas and 63.5% steam to a natural gas–steam mixture with a molar ratio of 2.5 (steam: natural gas). The flows of natural gas and steam were kept constant, while the flow of carbon dioxide was reduced from 1.88 kg_{CO_2}/h (427 mol_{CO_2}/h) to zero after 1 h. As can be seen, the gas composition changes during this interval to its new stationary value. After a further 15 h, the hydrogen concentration increases and the methane concentration decreases suddenly. A closer examination of this effect indicates that the change in composition is complete after 4 min. Within this period, the temperature at the process gas outlet drops from 1043 to 1038 K due to the better catalyst activity. Considering the change in methane conversion, the data analysis results in an increase from 18.4% during the blending experiment up to 27.2% for natural gas and steam with a transient step of 21.5% at 14 h. This leads to the conclusion that carbon dioxide blocks active sites of the catalyst even for several hours after total cessation of the carbon dioxide flow. The desorption process of carbon dioxide takes a long purge time.

Table 5 shows the product gas compositions after pre-reforming different natural gas–steam mixtures at methane conversion rates of 24% (27.1%) and 42.5% in comparison to a simulated anode gas recycling. The methane concentration increases with decreasing methane conversion rate, while the carbon dioxide concentration increases with increasing recycling ratio $R_{recycling}$. The influence of these gas compositions on the internal reformer will be the subject of a future investigation.

Another aspect of the catalytic steam-reforming process concerns CO production. In Fig. 10, the measured carbon monoxide concentrations are shown together with their equilibrium values. In this calculation, only the shift reaction is in equilibrium; the methane conversion rate is fixed at the experimental data point. As can be seen, the measured CO concentrations are somewhat higher than the calculated data. This is an indication that methane is first reformed into hydrogen and carbon monoxide. The conversion of carbon monoxide to carbon dioxide is kinetically

Table 5
Gas composition of the process gas at the pre-reformer outlet in different cases

Mix	T (K)	ξ_{CH_4}/ %	y_{CH_4}/ %	y_{H_2}/ %	y_{CO_2}/ %	y_{CO}/ %	y_{H_2O}/ %	$R_{recycling}$
NG-H_2O	955	24.3	15.2	27.5	6.6	1.35	48.1	–
NG-H_2O	1038	27.1	14.6	27.6	6.1	1.9	48.2	–
MIX D	963	9.9	18.2	16.8	12.1	1.7	49.6	0.43
MIX D	1029	16.9	16.3	20.8	12.0	2.8	46.5	0.43
NG-H_2O	955	42.5	11.5	42.6	8.5	3.9	32.6	–

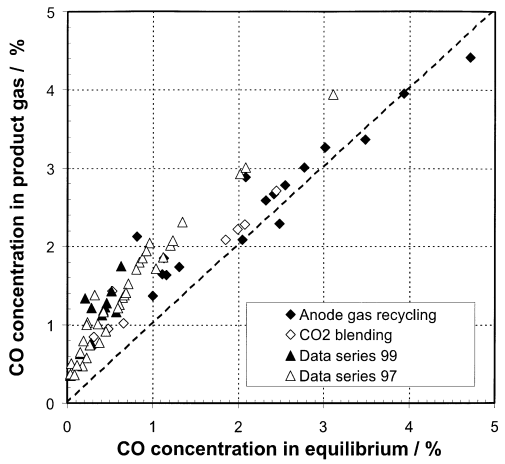

Fig. 10. Measured carbon monoxide concentration relative to the values calculated for the shift equilibrium.

controlled, so that the product gas does not reach the composition given by the shift equilibrium due to the limited amount of catalyst in the pre-reformer. If CO_2 is injected, i.e., in the case of anode gas recycling or CO_2 blending, the CO concentration approaches that of the shift equilibrium as shown in Fig. 10. The addition of CO_2 reduces the amount of CO which must be converted into CO_2 to reach the shift equilibrium. A more detailed presentation of the data is not possible due to the limited data points and the observed ageing effects. In principle, the carbon monoxide concentration increases with increasing methane conversion up to 4% at 40% conversion (without anode gas recycling). The carbon monoxide concentration is higher in the case of anode gas recycling.

In summary, the pre-reformer must be chosen with twice as much catalyst mass in order to perform anode gas recycling at 950 K. This is only valid for the experiments performed under the conditions given above, i.e., carbon dioxide concentrations in the inflow of the pre-reformer between 8% and 13%. The corresponding recycling rates are very low and lead only to an amount of 50% ($R_{\text{recycling}} = 1$) and 30% ($R_{\text{recycling}} = 0.4$) steam which can be recovered by anode gas recycling. For this case, the reduction of the evaporator size is not advantageous. The wall area of the evaporator used is 0.25 m^2. If the amount of fresh stream is reduced to 50%, the evaporator demands 0.13 m^2. In contrast, the pre-reformer wall area would require an increase from 0.6 m^2 to 1.2 m^2. From the proposed recycling ratios in Table 1 and the measured rates of methane conversion for gas mixtures given in Table 3, it is clear that, with increasing carbon dioxide and carbon monoxide concentration (21% CO_2, 6% CO), the specific rate of methane conversion decreases more markedly. At 1030 K, methane conversion decreases from 0.46 kg/(m^2 h) (0.3% CO_2) to 0.41 kg/(m^2 h) for 13% CO_2, 3% CO (mix extension A in Table 3). The linear extension of this trend predicts a conversion rate of 0.37 kg/(m^2 h) at 21% CO_2 and 6% CO, i.e., a reduction of 20% in catalyst activity. The catalyst mass of the pre-reformer would need to be increased by a factor of 1.2. At lower temperatures, the effect of anode gas recycling is much more pronounced and cannot be extrapolated, e.g., up to concentrations of 21% CO_2 and 6% CO. The energetic aspects of anode gas recycling are discussed more in detail by Riensche and Fedders [7].

4.4. Dynamic behaviour

Further measurements relating to the dynamic behaviour of the pre-reformer were made to clarify the response times of the complete unit. Several load changes were performed. Fig. 11 shows a load change with a decrease in mass flow of methane from 1.3 to 1.0 $kg_{\text{natural gas}}$/h, i.e., 81.25 and 62.5 mol/h, respectively. These correspond to 32% and 28% of the maximum mass flow of the controller. For the test with a maximum flow of about 130 ml/h, the unit itself operates in a medium partial load range. As can be seen, the mass flow controller needs only 15 s to reach a mass flow with a deviation of 1% (relative) to the stationary value after 3 min. The product gas shows a delay of 30 s before starting to change its composition. After 3 min, the product gas composition has reached equilibrium. The concentrations in the dry product gas were determined with a IR Binos Analyzer system. The CH_4 concentrations observed correspond to a methanol conversion rate of 10.5% to 13.9% at 62.5 mol/h. During the load change, the temperatures at the process gas outlet were stable at 918 K. The CO concentration at the pre-reformer outlet only varies between 2.40% and 2.34%.

A further load change shown in Fig. 11 was carried out by increasing the mass flow from 1 to 1.75 $kg_{\text{natural gas}}$/h,

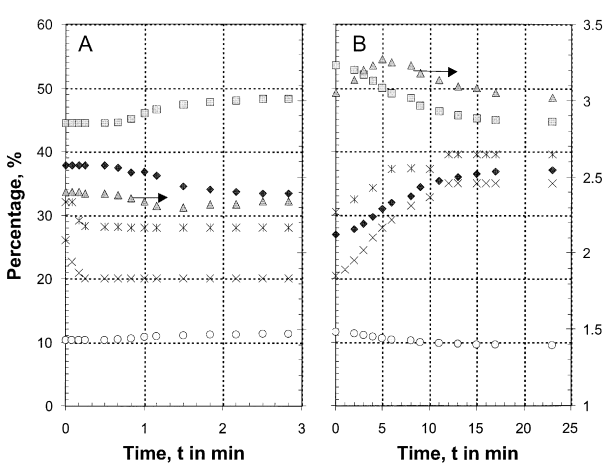

Fig. 11. Dynamic behaviour of a pre-reformer. (■) H_2; (♦) CH_4; (○) CO_2; (▲) CO; (×) FC($\dot{m}_{H_2O}$); (*) Y($\dot{m}_{H_2O}$). FC: mass flow measured by flow controller in percent; Y control value in percent. (A) Load change from 81.3 down to 62.5 mol/h at 918 K. (B) Load change from 62.5 up to 110 mol/h at 947 K.

i.e., an increase in molar flow from 62.5 to 110 mol/h. The partial load of the pre-reformer was increased from 50% to 87.5%. It can be observed that the reforming process is able to follow the load change given by the mass flow controller almost immediately. The controller completed the load change after 12 min, while the gas composition changed within 17 min. Also, the temperature was stable at 947 K. The corresponding methanol conversion rate changes from 24.5% to 18.3%.

4.5. Energy balance

A summary of the energy balances with respect to the pre-reformer and the evaporator/heat exchanger unit are given here. The analyses of the measured temperatures and concentrations provide the balance of enthalpy flows at the inlet and the outlet of the unit. A heat transfer coefficient can also be calculated from this data. It varies between 20–250 and 50 $W/(m^2\ K)$, on average, for the reformer. The heat transfer in the pre-reformer is influenced by the reaction rate and the flow through the Raschig rings. For the evaporator, an average heat transfer coefficient of 130 (90–200) $W/(m^2\ K)$ can be calculated.

The efficiency, in terms of enthalpy, for the heat exchange is about 90%, which is sufficient for a high temperature apparatus. The exergic efficiency can be calculated as 37%. Exergic losses originate from the chemical conversion, the heat transfer ($\Delta T_{ln,evaporator} = 120$ K; $\Delta T_{ln,reformer} = 81$ K for data series 97) and mixing with additional gases (H_2, CO, CO_2). Due to the ageing of the catalyst, the average temperature for the reformer drops to $\Delta T_{ln,reformer} = 53$ K from the data series 99.

These efficiencies are sufficient for a recuperative heat exchange using the waste heat of the exhaust gas coming from the afterburner and the SOFC (see Fig. 1). For a natural gas reformer connected to a polymer electrolyte fuel cell (PEFC) operating at 353 K, the heat must be provided by another kind of burner. In this case, the heat for the endothermic steam-reforming reaction and for steam production must be produced by a burner using residual amounts of hydrogen coming from the anode side of the PEFC and, in addition, natural gas. Such a system would resemble the test facility described in this paper. Taking the heat losses of the actual burner chamber into account as well, the efficiency decreases to 80%. Also, it has to be taken into account that the reforming process is incomplete in this case.

Efficiencies for components in fuel cell systems mostly relate the enthalpy flow of the hydrogen produced to the lower heating value of the energy carrier. In the case of an SOFC system, both hydrogen and carbon monoxide can be converted by electrochemical oxidation, so the efficiency of the pre-reformer expressed in terms of lower heating values for the incoming natural gas and the outgoing methane–carbon monoxide mixture amounts to 66%.

For the complete fuel processing system, electrical energy will also be consumed by the natural gas compressors. In the experiments (base 10 kW_{el} for the SOFC system) shown here, 2.27 kW ($\eta = 60\%$) is required to compress natural gas and air streams to a pressure of 3.5 bar. On the other hand, it is possible to use the enthalpy, i.e., 2 kW, by cooling the exhaust gas down to 353 K. By anode gas recycling, a heat value of 2 kW for pre-heating, evaporation and superheating of water can be saved. Unfortunately, anode gas recycling would require higher investment costs for a larger pre-reformer. A more detailed evaluation needs to be made in order to consider the complete system with all peripheral components.

5. Summary

A compact pre-reformer (10 kW) with Rashig ring layers was constructed and operated with natural gas. At 948 K and an outflow of 132.7 $mol_{natural\ gas}/h$, i.e., a mass flow of 2.1 $kg_{natural\ gas}/h$, a methane conversion of 22% and an ethane conversion of 46% were observed. No higher hydrocarbons were detected in the product stream.

Anode gas recycling led to a considerable decrease of the methane conversion rate at medium temperatures of 948 K. At 1013 K, the effect of an addition of anode gas is not so pronounced. The decrease in methane conversion leads to the required catalyst mass, which is twice as great as without anode gas recycling for experiments at 950 K. Since the addition of simulated anode gas had to be reduced relative to the data proposed by Riensche and Fedders [7], the catalyst mass could be higher by a factor of 1.2 at 1030 K. At lower temperatures and high recycling factors between 4 and 5, anode gas recycling does not seem to be efficient.

The tests of the pre-reformer show that a compact construction is technically feasible. Unfortunately, the ethane conversion is too low, i.e., the wet ethane product gas concentration amounts to about 1% and in addition, CO_2 blocks active catalyst sites. The effect of CO_2 on the catalyst surface is observed even hours after switching off the carbon dioxide addition. The dynamic behaviour and the technical performance of the pre-reformer, as well as the evaporator/heat exchanger unit, are adequate.

Acknowledgements

The authors thank St. von Andrian, B. Sobotta and W. Beckers for their contribution.

References

[1] E. Riensche, J. Meusinger, U. Stimming, G. Unverzagt, J. Power Sources 71 (1998) 306–314.
[2] E. Riensche, U. Stimming, G. Unverzagt, J. Power Sources 73 (1998) 251–256.
[3] G. Unverzagt, PhD Thesis, RWTH Aachen, 1995.

[4] J. Meusinger, E. Riensche, U. Stimming, J. Power Sources 71 (1–2) (1998) 315–320.
[5] E. Achenbach, E. Riensche, J. Power Sources 52 (1994) 283.
[6] W. Lehnert, J. Meusinger, E. Riensche, U. Stimming, in: B. Thorstensen (Ed.), Proc. 2nd Eur. SOFC Forum, Oslo, Norway, 1996, p. 143.
[7] E. Riensche, H. Fedders, Internal report of Forschungszentrum Jülich, IEV, Jül-2787, 1993.
[8] J.R. Rostrup-Nielsen, Catalytic Steam-Reforming, Springer, Berlin, 1984.
[9] H.G. Düsterwald, B. Höhlein, H. Kraut, J. Meusinger, R. Peters, Chem. Eng. Technol. 20 (1997) 617–623.